Published in final edited form as:
Early Hum Dev. 2008 March ; 84(3): 181–193. doi:10.1016/j.earlhumdev.2007.04.002.

Differentiation of xenografted human fetal lung parenchyma

Jelena Pavlovic[1], **Joanna Floros**[1,2,3,+], **David S. Phelps**[2], **Brian Wigdahl**[4], **Patricia Welsh**[4], **Judith Weisz**[3], **Debra A. Shearer**[3], **Alphonse Leure du Pree**[5], **Roland Myers**[5], and **Mary K. Howett**[3,4,+]

[1]Department of Cellular and Molecular Physiology, The Pennsylvania State University College of Medicine, Hershey, PA 17033, USA

[2]Department of Pediatrics, The Pennsylvania State University College of Medicine, Hershey, PA 17033, USA

[3]Department of Obstetrics and Gynecology, The Pennsylvania State University College of Medicine, Hershey, PA 17033, USA

[4]Department of Microbiology and Immunology, The Pennsylvania State University College of Medicine, Hershey, PA 17033, USA

[5]Department of Neuroscience and Anatomy, The Pennsylvania State University College of Medicine, Hershey, PA 17033, USA

Abstract

The goal of this study was to characterize xenografted human fetal lung tissue with respect to developmental stage-specific cytodifferentiation. Human fetal lung tissue (pseudoglandular stage) was grafted either beneath the renal capsule or the skin of athymic mice (NCr-nu). Tissues were analyzed from 3 to 42 days post-engraftment for morphological alterations by light and electron microscopy (EM), and for surfactant protein mRNA and protein by reverse transcription-polymerase chain reaction (RT-PCR) and immunocytochemistry (ICC), respectively. The changes observed resemble those seen in human lung development *in utero* in many respects, including the differentiation of epithelium to the saccular stage. Each stage occurred over approximately one week in the graft in contrast to the eight weeks of normal *in utero* development. At all time points examined, all four surfactant proteins (SP-A, SP-B, SP-C, and SP-D) were detected in the epithelium by ICC. Lamellar bodies were first identified by EM in 14 day xenografts. By day 21, a significant increase in lamellar body expression was observed. Cellular proliferation, as marked by PCNA ICC and elastic fiber deposition resembled those of canalicular and saccular *in utero* development. This model in which xenografted lung tissue in different stages of development is available may facilitate the study of human fetal lung development and the impact of various pharmacological agents on this process.

+Correspondence /Request for reprints: Joanna Floros, Ph.D., Evan Pugh Professor of Cellular and Molecular Physiology, Pediatrics, and Obstetrics and Gynecology, e-mail: jfloros@psu.edu, or Mary K. Howett, Ph.D., The Pennsylvania State University College of Medicine, 500 University Drive; Hershey, PA 17033, USA.
Current addresses: Mary K. Howett, Ph.D., Professor and Department Head, Bioscience and Biotechnology; RM118, Stratton Hall, Drexel University; Philadelphia, PA 19104, USA; e-mail: mkh28@drexel.edu
Brian Wigdahl, Ph.D., Professor and Chair, Department of Microbiology and Immunology, and Director, Institute for Molecular Medicine and Infectious Disease, Drexel University College of Medicine, Philadelphia, PA 19129, USA; e-mail: bw45@drexel.edu

Keywords

surfactant protein A (SP-A); SP-B; SP-C; SP-D; lamellar bodies; immunocompromised mice

Introduction

Development of a functional alveolar epithelium capable of gas exchange and surfactant secretion is essential for successful adaptation of the fetus to extra-uterine life. Because lung maturation is a late gestational event, respiratory distress is frequent in babies born prematurely. Premature infants are most commonly born during the saccular stage of lung development (26–34 wk of gestation) when lung pneumocytes are not yet completely differentiated. These infants often exhibit a deficiency of surfactant production that leads to insufficient gas exchange. Due primarily to a higher rate of multiple gestations, the overall number of premature live births (Mercer et al, 1999) has increased by 26% during the last three decades. This has lead to a significant increase in neonatal respiratory disease, including Respiratory Distress Syndrome (RDS) and Bronchopulmonary Dysplasia (BPD) (Clark et al, 2001; Jobe and Ikegami, 2000).

Premature birth is commonly marked by immaturity of the gas exchange regions, poorly developed blood supply, and a deficiency and perturbation of the surfactant system. Pulmonary surfactant is a lipoprotein complex produced by type II pneumocytes that acts to reduce surface tension at the air-liquid interface in the alveolus and thereby, prevent atelectasis (Floros, 1997; Phelps, 2001). Surfactant proteins (SPs) may contribute to surfactant function (SP-A, SP-B, SP-C) or associate with the surfactant complex but not contribute to its function (SP-D). Each SP has multiple important roles within the alveolus (Floros and Hoover, 1998; Phelps, 2001; Weaver and Whitsett, 1989) and is subject to developmentally- and hormonally-regulated expression (Ballard, 1984; Ballard et al, 1995; Dulkerian et al, 1996; Hoover et al, 1999; Karinch et al, 1998; Kumar and Snyder, 1998; Mendelson et al, 1991; Mendelson and Boggaram, 1991; Solarin et al, 1997; Wang et al, 2003). SP production starts early in development (pseudoglandular stage), but active secretion of functional surfactant (predominantly in the form of lamellar bodies) is initiated during the saccular stage of development, after almost 75% of gestation is completed (Ballard, 1984).

While lung development has been extensively studied in multiple models involving different animal species, studies of human lung development have primarily been limited to fetal lung explants (Ballard et al, 1995; Dulkerian et al, 1996; Karinch et al, 1998; Kumar and Snyder, 1998; Mendelson et al, 1991; Mendelson and Boggaram, 1991; Solarin et al, 1997). Although the importance of the fetal lung explant model is undisputed, the highly accelerated morphological development and limited viability of explants in cell culture (of the order of days) limits their use in studies of cellular and molecular changes specific for particular stages of lung development and studies over longer periods of time.

Models of organ development have been developed using immunocompromised mice as hosts for grafted fetal tissue (Cobb, 1975; Phillips and Gazet, 1969). Various xenograft models have been used extensively in cancer research to study mechanisms of carcinogenesis and the effects of different pharmacological agents on human tumor growth (Giovanella and Fogh, 1985; Malkinson, 2001), as well as in studies of transmission of infection in various tissues by pathogens (Howett et al, 1997; Howett et al, 1990; Howett et al, 1999; Kish et al, 2001; Kreider et al, 1985). With respect to lung embryogenesis, immunocompromised mice have been used to study whole organ lung development in mice (Schwarz et al, 2000; Vu et al, 2003), as well as lower (Groscurth and Tondury, 1982; Peault et al, 1994) and upper airway development in humans (Delplanque et al, 2000; Deutsch, 1997; Engelhardt et al, 1993; Filali et al, 2002; Pilewski et al, 1994; Puchelle and Peault, 2000). Allograft models have been used where whole

embryonic mouse lungs were grafted into severe-combined immunodeficient (SCID) mice (Schwarz et al, 2000; Vu et al, 2003). Progression of structural development as well as appearance of mature alveoli was observed 14 days after grafting. It has also been observed that (Phillips and Gazet, 1969) human fetal lung tissues grafted into a mouse treated with antilymphocytic serum (ALS, lymphocyte suppressing antibodies) could develop and grow in the host for up to 90 days. Others observed differentiation of lung-specific cell types in two, five, and eight week old transplant grafts (Groscurth and Tondury, 1982). More recently, a number of studies involving xenograft models of human upper airway development, have been reported (Delplanque et al, 2000; Puchelle and Peault, 2000). The focus in these studies was on the development of bronchial xenografts to study the pathogenesis of cystic fibrosis (Engelhardt et al, 1993; Filali et al, 2002). Although these studies have clearly shown that human embryonic lung tissue can be successfully differentiated in immunocompromised mice, the focus was on the endpoint of tissue development, rather than on the characterization of developmental processes.

Our goal was to characterize a model for the study of successive stages of development of the human lower airways, with particular emphasis on the expression of surfactant components. Based on the knowledge available from a number of lung xenograft models (Cobb, 1975; Delplanque et al, 2000; Deutsch, 1997; Engelhardt et al, 1993; Filali et al, 2002; Groscurth and Tondury, 1982; Peault et al, 1994; Phillips and Gazet, 1969; Pilewski et al, 1994; Puchelle and Peault, 2000; Schwarz et al, 2000; Vu et al, 2003), we hypothesized that human fetal lung parenchyma grafted into immunocompromised mice will undergo changes that mimic the stages of *in utero* lung development in many respects. The assumption was that although grafted tissue may undergo accelerated maturation, this acceleration would not be as rapid as that seen in fetal lung explants, enabling one to study stage-specific processes of lung development. In the present study, we characterized these stage-specific processes with respect to the progressive cytodifferentiation of a model of human fetal lower airway development.

Material and Methods

Fetal lung xenografts

Six to fourteen week-old female NCr-nu (nude) (Taconic Farms, Germantown, NY) were used for both renal subcapsular and subcutaneous grafts. Animals were maintained under pathogen-free conditions and were fed sterilized rodent Purina 5K52 diet. Research involving all animals followed the “Guiding Principles in the Care and Use of Animals” by the Council of the American Physiological Society and was approved by The Penn State College of Medicine Institutional Animal Care and Use Committee. Human fetal lung tissues (n=5), ranging from 13 to 17 weeks of gestation, were obtained from legal abortions where written informed consent was obtained according to a protocol approved by the Penn State College of Medicine Institutional Review Board. Fetal age was obtained from clinical information and confirmed by fetal foot-length measurements. To ensure that graft tissue was derived from fetal lung, only whole lung lobes were used for preparation of xenograft tissue. Fresh lower airways were cut under sterile conditions into 1-3 mm^3 pieces. Surgery was performed on nude mice anesthetized by intraperitoneal injection of 100 mg/kg Ketaset and 5 mg/kg Xylazine. Human fetal lung tissue was placed either under the dorsal fold of skin (four pieces) or beneath the renal capsule of each mouse (one piece). Xenografts were harvested 3-42 days after grafting. Mice were anesthetized with halothane and sacrificed by cervical dislocation.

Histology

Tissue harvested at 3, 6, 10, 14, 21, 28, 35 and 42 days after grafting was rapidly removed from the mouse skin or kidney, formalin fixed, and paraffin embedded. Tissues were cut into 4 μm thick sections and stained with hematoxylin and eosin for morphological examination. Using

light microscopy, tissue sections were examined for morphological characteristics of lung development. All tissues were examined independently and together by at least two researchers, who assigned the developmental stage to each section. The sections were viewed using a Nikon Eclipse E600 microscope and recorded using either a Spot digital camera (Diagnostic Instruments, Inc.) and Image Pro Plus version 3.0 software or a Nikon Digital Camera DXM 1200 and Nikon, ACT1 version 2 software.

Elastic fiber staining

Verhoff's-van Gieson's staining was performed as previously described (Tassler et al, 1994).

Electron microscopy

Xenograft tissues were fixed for 3 hr in 2% glutaraldehyde in 85 mM cacodylate buffer at room temperature, and post-fixed overnight in buffered osmium tetroxide (1%) at 4°C. Following dehydration in graded ethanol, the tissue was infiltrated with propylene oxide and EMbed 812. After an overnight rotation in propylene oxide: EMbed 812 (1:1), tissues were rotated and embedded in 100% EMbed 812. Semi-thin sections were stained with toluidine blue and examined under a light microscope. If the sections appeared satisfactory by light microscopy, blocks were mounted and sectioned on a Sorvall MT2-B ultramicrotome at 0.08 μm (800Å) in preparation for electron microscopy. These ultra thin sections were mounted on square 200 mesh copper grids, stained with uranyl acetate and lead citrate and examined with a Philips 400 transmission electron microscope.

Immunocytochemical Analyses (ICC)

Formalin-fixed, paraffin-embedded tissue sections were deparaffinized and stained for the presence of human SPs using the following rabbit polyclonal antibodies: anti-SP-A (1:250) (Phelps and Floros, 1991), anti-SP-B (1:250, Chemicon, Temecula, CA), anti-pro-SP-C (1:100, Chemicon), and anti-SP-D (1: 500, Chemicon). A low-temperature antigen retrieval procedure (Brown, 1998) was applied to deparaffinized and rehydrated tissue sections using 0.1 mol/L citrate buffer, pH 6.0, for 1 hr at 80°C followed by dehydration and rehydration by incubation in xylene and graded ethanol series. Endogenous alkaline phosphatase was inhibited by immersing the slides in 0.2 N HCl for 5 min. Samples were blocked with 15% normal goat serum (Vector Laboratories, Burlingame, CA) in 1× PBS and 0.3% TX-100. Following overnight incubation at 4°C with each selected primary antibody, tissue sections were incubated with biotinylated goat anti-rabbit secondary antibody for 1 hour at room temperature. All subsequent steps were performed at room temperature. The signal from the secondary antibody was visualized using Vectastain ABC with alkaline phosphatase as the reporter, and Vector Red Alkaline Phosphatase Substrate Kit I reagent (Vector Laboratories, Burlingame, CA) as the chromogen.

For ICC with anti-human antibodies to proliferating cell nuclear antigen (PCNA) and endothelial cell markers PECAM-1 (same as CD31), Mouse on Mouse DAKO Ark kit (DAKOCytomation, Carpinteria, CA) was used as per manufacturer's instructions. Both primary antibodies (anti-human PCNA and anti-human CD31) were mouse monoclonal antibodies that are specific for the human antigen. The primary antibodies (PCNA 1:50, and CD31 1:20, DAKOCytomation) were pre-incubated with the secondary antibody in equimolar amounts in order to avoid the staining of mouse immunoglobulin within the human grafts with the secondary anti-mouse IgG antibody. Control mouse tissues were negative for PCNA and CD31 staining using this protocol (not shown). Images of tissue sections were captured as described above.

Reverse Transcription-Polymerase Chain Reaction (RT-PCR)

RNA was isolated from snap-frozen, non-fixed fetal lung tissue, graft tissue, and adult human lung tissue (obtained from pneumonectomies performed at Hershey Medical Center), using the Qiagen RNeasy Mini Kit (Qiagen, Valencia, CA). Briefly, tissue was first disrupted using a hand held mortar and pestle, homogenized in Qiashredder, and processed as described by the manufacturer. Extracted RNA (1 μg of each sample) was DNase I treated and reverse transcribed using a gene-specific oligonucleotide (oligo) for each surfactant protein (see below). The RT procedure was performed as described previously (Karinch and Floros, 1995). RNA from human spleen tissue (Ambion, Austin, TX) was used as the negative control. The orientation, gene specificity, and nucleotide position of each oligo used in the present study are shown in Table 1. For SP-A, RT was performed using oligo 68A, followed by the first amplification with oligos 780/781, and 1 μl of this template was used for a nested reaction with primers 1321/781 resulting in a 100 bp long template. For SP-B, oligo 110 was used for RT, followed by a first cycle of PCR with oligos 70A/603, followed by nested PCR with oligos 172/189 to create a 51bp template. RT for SP-C was performed using oligo 86A, oligos 1108/1106A were used in the first round of PCR, while oligos 1108/1116 were used in the nested reaction producing a 142 bp long amplicon. Finally, oligo 961 was used for SP-D RT, followed by first round of PCR with oligos 825/925, and nested PCR with oligos 915/925 resulting in a 291 bp long template. All PCR reactions were performed using 4 μg cDNA from the gene-specific RT reaction in final concentrations of 0.5 × buffer 1 (Roche, Indianapolis, IN) and 0.5 × buffer 2 (Roche), 2 ng of each primer, 100 μM of each dNTP and 0.15 μl of Taq Polymerase (Roche). The PCR profile was as follows: one cycle of 95°C for 2 min, followed by 35 cycles of: 95°C for 30 seconds, 58°C for 1 min, and 72°C for 1 min, this was followed by one cycle of 72°C for 5 min. DNA fragments from the first PCR reaction were used for nested PCR, with the same PCR profile. Amplified SP gene-specific fragments were then resolved on 8% PAGE gels, and specific bands visualized.

Results

Both renal subcapsular and subcutaneous sites of engraftment support graft growth and development

Human fetal lung tissue from fetuses of 13 to 17 weeks of gestation was grafted underneath the renal capsule (subcapsular) or subcutaneously in nude mice and harvested after 3, 6, 10, 14, 21, 28, 35 and 42 days. Each mouse received only one type of graft.

Xenografts established at both transplant sites underwent lung development to the saccular stage (Fig. 1D). Subcutaneous grafts underwent substantial macroscopic growth with increased time of transplantation, at times reaching a volume of 4-5 mm^3. The increase in macroscopic size of subcapsular grafts was less, presumably due to the lack of space to grow (Fig. 1.II and Fig.1.I, respectively). Subcutaneous xenografts from the anterior part of the mouse back appeared to develop faster and initiate morphological changes by day three post-grafting, whereas such changes in the posterior grafts were observed at day six post-grafting. By six days post-grafting, the developmental progression of both anterior and posterior dorsal subcutaneous xenografts was equivalent to that of subcapsular grafts (Fig 1. CI and CII). Limiting the initial size of subcutaneous grafts to about 1 mm^3, minimized the lack of uniformity in tissue differentiation observed in larger grafts (not shown).

To ensure that a sufficient quantity of xenograft tissue was available for post-grafting analysis, three to four 1 mm^3 pieces were placed into each subcutaneous pocket on the back of the nude mouse. These were generally found to be fused together 2-4 weeks after grafting, contributing to the larger size of subcutaneous grafts. Our overall observations indicate that both subcutaneous and subcapsular grafts represent adequate models of human fetal lung tissue

development (Fig. 1.I and Fig. 1.II). However, subcutaneous grafts (Fig. 1.II) have the advantage of greater ease of engraftment, better access to graft tissue, and larger size of grafts.

Human fetal lung grafts mimic the sequential stages of lung development *in utero*

The starting tissue for both subcapsular and subcutaneous grafts was at the pseudoglandular stage of development (Fig. 1A). The progression of tissue grafts through subsequent stages of lung development was observed at different time points post-grafting. The pseudoglandular stage was characterized by the formation of conducting airways that were lined by cuboidal epithelium (Fig. 1B). There is a limited number of proliferating cells at this stage of development, as indicated by proliferating cell nuclear antigen (PCNA) immunoreactivity (Fig. 2B). Staining for collagen and elastic fibers with Verhoff's-van Gieson's stain shows a collagen-rich tissue lacking elastic fibers (Fig. 3A).

After 3 days of grafting, small increases in future alveolar spaces were observed as well as thinning of the epithelium, changes that represents the late pseudoglandular phase (Fig. 1B.III). Grafts harvested after 6 and 10 days of engraftment resemble the canalicular stage of lung development; six day old xenografts resembled the early canalicular stage, and 10 day old grafts had characteristics of late canalicular phase (Fig. 1C). During the late canalicular phase of lung development, lung acini were formed (Fig. 1C.III), and the numbers of capillaries visible in the mesoderm increased. The latter process was clearly visible by light microscopy, but not readily apparent in the corresponding photographic images. Appearance of early primary saccules was observed in 10 day grafts. This process was marked by a dramatic increase in PCNA-positive cells within the saccular spaces (Fig. 2D). Alveolar sacs in these grafts were lined by flattened cuboidal epithelium and closely resembled the morphological appearance of a 20+ week old human fetus (Copland and Post, 2004).

Fetal lung grafts harvested 14 and 21 days post-grafting resemble the early and late saccular stage, respectively. In these grafts, the epithelium was flattened, representing the differentiation of pre-type II cuboidal cells from the canalicular phase into maturing type II cells, and further differentiation of the type II cells into putative type I pneumocytes (Fig. 1D.III). Cellular proliferation was particularly evident in 14 day grafts based on PCNA immunostaining (Fig. 2E), while the 21 day grafts had very few PCNA immunopositive cells (Fig. 2F) indicating terminal differentiation of the tissue. As a result of cellular differentiation and the reduction of interstitial tissue, alveolar crests were formed and divided primary saccules into subsaccules or primitive alveoli (Fig. 1D.I and 1D.II). Elastic fiber deposition was seen in 14 day grafts as punctate dots at tips of developing alveolar crests (Fig. 3B). Elastic fibers were not apparent in all graft tissues (not shown) and were scarce in representative sections of 21 day grafts. Notably, there were no elastic fibers seen in 28 or 35 day old grafts. Ciliated and non-ciliated cells were observed in the conducting airways in these grafts. Moreover, a significant increase in the macroscopic growth of graft tissue was readily observed after 14 days of engraftment.

Human fetal lungs transplanted for longer than 28 days (up to 42 days) (Fig. 1E.I and 1E.II) had thin walls, with limited amounts of interstitium (Fig. 1E.III), suggesting their progression past the saccular stage of lung development. The airspaces were significantly enlarged compared to earlier time points, and were lined with flattened epithelium, presumably consisting of putative type I cells (Fig. 1E.III). Although the grafts developed in a limited space, particularly in the case of renal subcapsular grafts, alveolar spaces were never collapsed. The alveolar spaces were always opened and filled with fluid, presumably secreted by the lung tissue.

Lamellar bodies are present in graft tissue, consistent with *in utero* lung development

Based on light microscopy (Fig. 1), we conclude that the grafts follow time-dependent structural and morphological development. To determine whether these structural changes were also complemented by specific cellular and biochemical changes, grafts were examined by EM for the presence of lamellar bodies and surfactant proteins. The starting graft tissue in the pseudoglandular stage of development did not contain lamellar bodies, but had abundant glycogen stores, as indicated by the dense gray areas (arrow, Fig. 4.A2). As the glycogen stores started to diminish, lamellar bodies were detected in 14 day grafts. At the same time, morphological differentiation of the epithelium into mature type II pneumocytes was observed. Figure 4.B2 shows lamellar bodies (long arrow) and the apparent beginnings of microvilli (thick arrow) at the apical cell surface in the 14 day grafts, while Figure 4.C2 shows a significant increase in the number of lamellar bodies per cell (long arrow), and an abundance of microvilli on the apical membrane in the 21 day graft. Note that even though Fig. 4.C1 is at lower magnification than Fig. 4.B1, the abundant microvilli are readily detectable (area marked by a dotted line). Numerous secreted lamellar bodies and some unraveling of lamellar bodies were observed in the saccular spaces, but no tubular myelin structures (extracellular structural forms of surfactant) were observed in graft tissue. Overall, these images closely resemble the progression of pneumocyte differentiation during *in utero* lung development.

Surfactant proteins are present in graft tissue, consistent with *in utero* lung development

mRNA for all four proteins was present in the starting fetal lung at 16 weeks of gestation and message persisted during the graft development (not shown). However, adequate quantification of mRNA across the developmental stages could not be done due to the heterogeneity and sampling of the xenograft tissue and the fact that RT-PCR does not provide a quantitative measure. In order to study the pattern of SP expression throughout graft development, all time points of graft transplantation were examined for the presence of SPs by ICC. Starting fetal tissue was positive for all four SPs as assessed by ICC using a specific antibody for each SP (Fig 5). Pre-type II cells of early graft time points (3, 6, 10, 14, and 21 day grafts) showed a presence of all four SPs. Figure 6 shows 21 day grafts for all of the proteins.

Localization of SP-D was limited to the apical surface of cells, whereas SP-A, SP-B, and SP-C displayed more uniform patterns of distribution within the cell (Fig. 5 and Fig. 6, insert). It is of interest that on one occasion, ciliated cells of conducting airways in addition to type II pneumocytes were also found to express SP-D by ICC. Although these cells were immunonegative for other SPs, a number of other cells of unknown type were seen to be positive for all four SPs as determined by ICC. Moreover, post-translational processing and modification of the primary translation products to more mature and multimeric forms of SP-A or SP-D could not be studied due to the limited amount of tissue available.

We speculate that these cells are in intermediary stages of development of known and readily identifiable lung cell types. As cytodifferentiation progressed, SP-positive pre-type II cells differentiated into type II cells that further differentiated into putative type I cells and the number of SP-A, SP-B, SP-C, and SP-D positive cells per terminal airway decreased. Figure 7 depicts SP-A ICC at various graft time points (6, 10, 14, and 28 day grafts).

Blood vessels are present in the grafts as shown by ICC for human PECAM-1

In order to assess the vascularization of the subcutaneous grafts and origin of blood supply within the grafts, sections were immunostained with endothelial cell marker PECAM-1 specific for human antigen. In 3 day grafts, a network of blood vessels immunopositive for PECAM-1 was observed within the mesenchyme as shown in Fig. 8A (arrows). With the progression of tissue differentiation, thinning and branching of the PECAM-1 immunopositive vessels (arrowhead) was seen in the 6 day (Fig. 8B) graft. PECAM-1 staining was considerably

decreased in all other graft time points. By 14 days staining was predominantly visible in the subpleural areas, as shown in Fig. 8C. There was undetectable or very little human PECAM-1 positive staining visible in the interstitium of later graft time points.

Together, these observations indicate that human fetal lower airways grafted under renal capsule and subcutaneous tissues of nude mice can provide a model for study of human fetal lung development.

Discussion

Although a number of experimental models for the study of human fetal lung development are available, we undertook the current study to establish and characterize a model that could parallel normal intrauterine lung development in a time course more amenable to the study of stage-specific lung development. The goal of our study was to extend the characterization of currently available models and characterize a human fetal lung xenograft model, where successive stages of lung development could be studied with respect to morphological changes characteristic of cellular differentiation and the expression of the surfactant system. We observed that fetal lungs grafted under the renal capsule or subcutaneously in nude mice undergo maturation and differentiation where SPs and lamellar bodies are produced in a cell- and developmental stage-specific manner.

Overall macroscopic growth was observed in both types of grafts with increasing engraftment time, and this was particularly pronounced in subcutaneous grafts. Given the size restrictions of graft tissue, measurements of weight for comparisons of dry and wet tissue weights were impractical, although larger grafts were noted to have more lung fluid by gross observation. A considerable increase in the size of grafts after longer grafting times has been observed in both renal subcapsular (Vu et al, 2003) and subcutaneous (Cobb, 1975; Groscurth and Tondury, 1982; Peault et al, 1994; Phillips and Gazet, 1969) mouse fetal lung allograft models, although a comparison of these two engraftment sites has not been done previously. In the present study, initial transplantation of smaller pieces at both graft sites (subcapsular and subcutaneous) resulted in a more rapid vascularization of the entire area of the graft tissue and thus uniform growth and differentiation. The greater abundance and uniformity of blood supply to all cellular structures in smaller grafts are presumed to eliminate initial necrosis at early graft time points and prevent disruption of development in later time points.

The xenograft model characterized in the present study offers advantages over the fetal lung explant model, because the development of the xenografted tissues is conducive to stage-specific studies. Although xenograft development is accelerated compared to *in utero* development, in this model each developmental stage occurs over one week. This one week interval makes it amenable to the study of stage-specific cellular and biochemical processes. A comparative study of fetal lung explant and mouse renal subcapsular fetal lung allograft models showed the advantages of the latter. While mouse fetal lung grafts undergo extensive proximal and distal differentiation of the epithelium that follows closely the temporal differentiation *in utero*, the lung explant cultures rapidly undergo branching morphogenesis at first (after 3 days), but after longer times in culture (5 days) cease development and start to deteriorate (Vu et al, 2003).

Factors responsible for the accelerated lung development observed *in vitro* and/or *in vivo* are not known. Removal of tissue from putative inhibitory factor(s) present *in utero* is a possible explanation (Gross, 1983). Moreover, cellular and biochemical changes of lung structure may be under tight microenvironmental and hormonal control, and any changes in these conditions may have downstream effects on lung development (Ballard, 1984; Mendelson and Boggaram, 1991). Estrogen is known to be one of the regulators of fetal lung development and surfactant

synthesis. However, in studies where production of estrogen was suppressed in pregnant baboons (Pepe et al, 2003) the fetal lungs continued to grow and exhibited normal morphology. Moreover, female nude mice had relatively low levels of primary estrogens compared to human females (Witorsch, 2002), indicating that the accelerated lung development may not be due to the estrogen status of nude mice, but perhaps to other factors not yet well understood.

However, although tissue differentiation was accelerated compared to the *in utero* time scale, the changes in tissue morphology resembled the stages of human *in utero* lung development (pseudoglandular, canalicular and saccular). Each stage of lung development (about 8 weeks of *in utero* development) appeared to require about one week of graft development, with grafts reaching the early saccular stage after 14 days of engraftment. This is in contrast to the previous studies that have examined human graft development at multiple time points. In one study where fetal lungs from 10-14 weeks of gestation were subcutaneously grafted into nude mice, grafts resembling canalicular stage of development were observed at 8 weeks post-grafting (Groscurth and Tondury, 1982). The time course of tissue differentiation also appears to be accelerated in the present model, as compared to another study where fetal lungs ranging from 8-12 weeks of gestation were grafted for 3, 6, 11, and 19 weeks (Peault et al, 1994). Saccular stage-like changes were observed in 11 weeks post-engraftment as compared to 3 weeks in our study. The accelerated timing observed in the present study is comparable to the subcutaneous mouse allograft model, where E14.5 mouse fetal lungs required two weeks to differentiate to the saccular stage (Schwarz et al, 2000). On the other hand, both of these are in contrast to the renal subcapsular mouse allograft model (Vu et al, 2003), where timing of developmental stages of E12.5 mouse embryonic lungs closely follows that of *in utero* development. The observation that renal subcapsular lung allografts develop faster than the subcutaneous grafts suggests that the extra space provided for subcutaneous graft development and extra fluid accumulation within these grafts are not key factors in tissue development.

Differences in timing are probably due to a number of factors. Whether differences in developmental timing are dependent on the starting gestational age in human lung development is still unclear. Studies of human fetal grafts focusing on the end-point of fetal lung development (i.e. structural morphogenesis and appearance of alveolar-like structures) resemble the longer time points of our model (>28 days of grafting) with expanded alveoli that are presumably fluid-filled. Human fetal lung rudiments from 7.5 to 16 weeks grafted subcutaneously into SCID mice all showed mature bronchioles and alveoli after 6-8 weeks, regardless of their starting gestational age (Peault et al, 1994). This argues against a significant role of the starting gestational age in timing of lung development in these models.

Lung epithelial differentiation and branching are intimately tied to vascularization of the lung. Vascular development in the embryonic lung takes place through two simultaneous mechanisms. Angiogenesis is characterized by budding and branching of new vessels and their invasion of the pulmonary parenchyma, while vasculogenesis occurs by differentiation and organization of endothelial cells in lung mesenchyme that is necessary for the coordinated development of airways and blood vessels (deMello et al., 1997). Since blood vessels are formed in coordination with the epithelium and the epithelial branching is determined by epithelial-mesenchymal interactions, differentiation of epithelial cells in the model should be accompanied by changes in vasculature. In the present study, endothelial cell changes as assessed by human antigen specific endothelial cell marker PECAM-1, suggest significant remodeling over the course of differentiation of the graft. As tissue differentiation progressed and endothelial cells became more attenuated, the PECAM-1 staining became less intense. In later day grafts (≥14 days), PECAM-1 immunopositive structures persisted in subpleural areas, however the staining was virtually absent from the extensively remodeled interstitium. In the areas where interstitium had been extensively remodeled and reduced in mass, with evidence

of continued differentiation of the epithelium and active cell division, and no evidence of necrosis, no PECAM-1 staining was observed.

Since graft tissue can not continue to be viable, differentiate, and grow without a blood supply, it is reasonable to deduce that at later time points host angiogenesis may be sufficiently developed to infiltrate the graft, and in turn take over the support of its growth. Studies in mouse allograft models have provided evidence for both sources of blood supply to the graft. While Schwartz et al. showed that the grafts were vascularized by vessels originating from endogenous endothelial cells, Vu et al. observed that host blood vessels provide circulation to the graft in addition to that of endogenous endothelial structures. The present PECAM-1 ICC data support the notion that graft endogenous endothelial cells are initially present and at later stages of development these are replaced by host vascular structures. Mechanisms of embryonic vasculogenesis are poorly understood. It is possible that in the later stages of graft development, where extensive remodeling has already taken place, the reservoir of native graft (human) endothelial stem cells becomes depleted and the host vasculature has had sufficient time to completely penetrate the tissue and thus provide the blood supply needed to support further growth and differentiation of the grafted tissue.

Both mRNA and protein of all four SPs were expressed in the starting fetal lung tissues, and their expression was preserved during graft development. The presence of SPs in tissues of early graft time points and therefore in pre-type II cells was observed by immunostaining, in open airways throughout the lung. However, with progression of gestation the relative number of SP-positive cells per terminal air space decreased, as the SP-positive pre-type II cells differentiated into SP-negative type I cells. This is in agreement with reported findings (Vu et al, 2003) in the mouse renal subcapsular model, where a decrease in a number of pro-SP-C-positive cells with developmental progression of tissues was observed.

There has been an apparent discrepancy in the literature regarding the expression patterns of SPs during development. The assumption has been that SP-B and SP-C are not found in human fetal tissues until about 18-20 weeks of gestation, and that SP-A and SP-D are not expressed until about 24-26 weeks of gestation (Ballard, 1984; Ballard et al, 1995; Mendelson et al, 1991; Mendelson and Boggaram, 1991). These observations differ from results in the present study and a number of other recent studies where expression of these proteins was observed either in early or late pseudoglandular phase of development. Expression of SP-A and SP-D has been observed as early as 10-12 weeks of human gestation (Otto-Verberne et al, 1990; Stahlman et al, 2002), while after 15 weeks of gestation expression of all four proteins has been readily detected in a number of studies (Dulkerian et al, 1996; Khoor et al, 1993; Khoor et al, 1994; Solarin et al, 1997; Wang et al, 2003). Because the focus in these studies was on the identification of SPs in tissues of various gestational ages and not on the functions of these proteins, it is currently unknown whether the presence of these proteins at such early time points in gestation has any functional significance. The time interval between tissue procurement and experimentation, as well as the method of birth termination may be some of the factors contributing to the above-mentioned discrepancies in SP expression. The time interval between tissue procurement and experimentation, in the present study was rather short (three to eight hours).

Normal fetal lung development is dependent on sustained lung expansion due to the presence of lung fluid. Tracheal obstruction in animal models has been shown to accelerate fetal lung growth (Alcorn and Mendelson, 1993; Piedboeuf et al, 1997). Conditions that are associated with lung liquid drainage are characterized by pulmonary hypoplasia and an excess of type II cells (Flecknoe et al, 2003; Laudy and Wladimiroff, 2000). Hypoplasia is reversible with tracheal ligation, where presumed accumulation of lung fluid induces rapid lung growth and changes in alveolar structure (Flecknoe et al, 2000). In order to differentiate between the actual

cellular growth of the graft vs. the increase in size due to fluid accumulation and/or fusion of grafts, ICC for proliferation marker (PCNA) was performed. Although, the xenograft model, described in the present study, resembles models of tracheal obstruction with respect to microscopic changes and dilatation of alveoli observed at longer times of engraftment, the cellular proliferation patterns of graft tissues are more similar to those of control animals than to those of tracheal occlusion animals (Maltais et al, 2003). Compared to animals with tracheal obstruction showing a rapid increase in proliferation after 36 hours, lung grafts initially have slightly increased proliferation rates (as shown by PCNA immunopositivity) followed by higher rates of proliferation after 10 and 14 days of engraftment. Therefore, according to the presence of PCNA immunopositive cells, proliferation of graft tissues is most prominent in the canalicular and saccular stage, indicative of actual and stage appropriate tissue differentiation and growth. Tracheal obstruction is also marked by increased elastin synthesis and tissue deposition (Joyce et al, 2003). In contrast to this, in our model elastic fibers were found only at the tips of the developing alveolar secondary crests, as seen during *in utero* development. Moreover, the appearance and secretion of energy-demanding, highly-regulated cellular organelles such as lamellar bodies, specific for the type II pneumocyte, further underscores the similarity of graft development to *in utero* development.

In summary, through morphological and biochemical analysis of fetal lung tissue development, we were able to show that cytodifferentiation of human fetal lung xenografts resembles stages of human *in utero* development. This model is likely to serve as a valuable tool for the study of specific stages of human lung development and the temporal and spatial changes in expression and regulation of surfactant proteins through different stages.

Acknowledgments

The authors wish to thank Lynn Budgeon and Shendra Miller for technical assistance, and Dr. Gary Clawson for the use of the digital microscope. This work was supported by NIH RHL34788, PHS PO1 AI 37829, and CA 54559. Jelena Pavlovic is an MD/PhD student and Dr. Joanna Floros is her thesis advisor.

References

Alcorn JL, Mendelson CR. Trafficking of surfactant protein A in fetal rabbit lung in organ culture. Am J Physiol 1993;264:L27–35. [PubMed: 8430814]

Ballard PL. Combined hormonal treatment and lung maturation. Semin Perinatol 1984;8:283–292. [PubMed: 6093266]

Ballard PL, Nogee LM, Beers MF, Ballard RA, Planer BC, Polk L, deMello DE, Moxley MA, Longmore WJ. Partial deficiency of surfactant protein B in an infant with chronic lung disease. Pediatrics 1995;96:1046–1052. [PubMed: 7491219]

Benson B, Hawgood S, Schilling J, Clements J, Damm D, Cordell B, White RT. Structure of canine pulmonary surfactant apoprotein: cDNA and complete amino acid sequence. Proc Natl Acad Sci U S A 1985;82:6379–6383. [PubMed: 3863100]

Brown C. Antigen retrieval methods for immunohistochemistry. Toxicol Pathol 1998;26:830–831. [PubMed: 9864103]

Chinoy MR, Miller SA, Myers RL, Cilley RE, Dillon PW. Persistent vascular defects in lung allografts attributed to defective endogenous endothelial progenitors. J Surg Res 2005;124(1):14–22. [PubMed: 15734474]

Clark RH, Gerstmann DR, Jobe AH, Moffitt ST, Slutsky AS, Yoder BA. Lung injury in neonates: causes, strategies for prevention, and long-term consequences. J Pediatr 2001;139:478–486. [PubMed: 11598592]

Cobb LM. Growth and development of human fetal trachea and lung in immune-deprived mice. Thorax 1975;30:357–359. [PubMed: 1096353]

Copland I, Post M. Lung development and fetal lung growth. Paediatr Respir Rev 2004;5:S259–264. [PubMed: 14980282]

Crouch E, Rust K, Persson A, Mariencheck W, Moxley M, Longmore W. Primary translation products of pulmonary surfactant protein D. Am J Physiol 1991;260:L247–253. [PubMed: 1708210]

Delplanque A, Coraux C, Tirouvanziam R, Khazaal I, Puchelle E, Ambros P, Gaillard D, Peault B. Epithelial stem cell-mediated development of the human respiratory mucosa in SCID mice. J Cell Sci 2000;113(Pt 5):767–778. [PubMed: 10671367]

deMello DE, Sawyer D, Galvin N, Reid LM. Early fetal development of lung vasculature. Am J Respir Cell Mol Biol 1997;16:568–581. [PubMed: 9160839]

Deutsch G, H B, Huff D, Ptt B, Pilewski J. Transcription factors in human fetal pulmonary epithelium and developing xenografts (Abstract). Am J Respir Crit Care Med 1997;155

Dulkerian SJ, Gonzales LW, Ning Y, Ballard PL. Regulation of surfactant protein D in human fetal lung. Am J Respir Cell Mol Biol 1996;15:781–786. [PubMed: 8969273]

Engelhardt JF, Yang Y, Stratford-Perricaudet LD, Allen ED, Kozarsky K, Perricaudet M, Yankaskas JR, Wilson JM. Direct gene transfer of human CFTR into human bronchial epithelia of xenografts with E1-deleted adenoviruses. Nat Genet 1993;4:27–34. [PubMed: 7685651]

Filali M, Zhang Y, Ritchie TC, Engelhardt JF. Xenograft model of the CF airway. Methods Mol Med 2002;70:537–550. [PubMed: 11917549]

Flecknoe S, Harding R, Maritz G, Hooper SB. Increased lung expansion alters the proportions of type I and type II alveolar epithelial cells in fetal sheep. Am J Physiol Lung Cell Mol Physiol 2000;278:L1180–1185. [PubMed: 10835323]

Flecknoe SJ, Wallace MJ, Cock ML, Harding R, Hooper SB. Changes in alveolar epithelial cell proportions during fetal and postnatal development in sheep. Am J Physiol Lung Cell Mol Physiol 2003;285:L664–670. [PubMed: 12794005]

Floros J, Hoover RR. Genetics of the hydrophilic surfactant proteins A and D. Biochim Biophys Acta 1998;1408:312–322. [PubMed: 9813381]

Floros, J.; Phelps, DS. Pulmonary surfactant. In: Yaksh, T.; Lynch, C., III; Zapol, WM.; Maze, M.; Biebuyck, JF.; Saidman, LJ., editors. Anesthesia: Biologic Foundations. Lippincott-Raven; Philadelphia: 1997. p. 1259-1279.

Giovanella BC, Fogh J. The nude mouse in cancer research. Adv Cancer Res 1985;44:69–120. [PubMed: 3898740]

Glasser SW, Korfhagen TR, Perme CM, Pilot-Matias TJ, Kister SE, Whitsett JA. Two SP-C genes encoding human pulmonary surfactant proteolipid. J Biol Chem 1988;263:10326–10331. [PubMed: 2839484]

Groscurth P, Tondury G. Cytodifferentiation of human fetal lung tissue following transplantation into “nude” mice. Anat Embryol (Berl) 1982;165:291–302. [PubMed: 6760745]

Gross I. The regulation of fetal lung development. Prog Clin Biol Res 1983;140:93–102. [PubMed: 6369344]

Hoover RR, Thomas KH, Floros J. Glucocorticoid inhibition of human SP-A1 promoter activity in NCI-H441 cells. Biochem J 1999;340(Pt 1):69–76. [PubMed: 10229660]

Howett MK, Christensen ND, Kreider JW. Tissue xenografts as a model system for study of the pathogenesis of papillomaviruses. Clin Dermatol 1997;15:229–236. [PubMed: 9167907]

Howett MK, Kreider JW, Cockley KD. Human xenografts. A model system for human papillomavirus infection. Intervirology 1990;31:109–115. [PubMed: 2165039]

Howett MK, Neely EB, Christensen ND, Wigdahl B, Krebs FC, Malamud D, Patrick SD, Pickel MD, Welsh PA, Reed CA, Ward MG, Budgeon LR, Kreider JW. A broad-spectrum microbicide with virucidal activity against sexually transmitted viruses. Antimicrob Agents Chemother 1999;43:314–321. [PubMed: 9925525]

Jobe AH, Ikegami M. Lung development and function in preterm infants in the surfactant treatment era. Annu Rev Physiol 2000;62:825–846. [PubMed: 10845113]

Joyce BJ, Wallace MJ, Pierce RA, Harding R, Hooper SB. Sustained changes in lung expansion alter tropoelastin mRNA levels and elastin content in fetal sheep lungs. Am J Physiol Lung Cell Mol Physiol 2003;284:L643–649. [PubMed: 12618425]

Karinch AM, Deiter G, Ballard PL, Floros J. Regulation of expression of human SP-A1 and SP-A2 genes in fetal lung explant culture. Biochim Biophys Acta 1998;1398:192–202. [PubMed: 9689918]

Karinch AM, Floros J. 5′ splicing and allelic variants of the human pulmonary surfactant protein A genes. Am J Respir Cell Mol Biol 1995;12:77–88. [PubMed: 7811473]

Khoor A, Gray ME, Hull WM, Whitsett JA, Stahlman MT. Developmental expression of SP-A and SP-A mRNA in the proximal and distal respiratory epithelium in the human fetus and newborn. J Histochem Cytochem 1993;41:1311–1319. [PubMed: 8354874]

Khoor A, Stahlman MT, Gray ME, Whitsett JA. Temporal-spatial distribution of SP-B and SP-C proteins and mRNAs in developing respiratory epithelium of human lung. J Histochem Cytochem 1994;42:1187–1199. [PubMed: 8064126]

Kish TM, Budgeon LR, Welsh PA, Howett MK. Immunological characterization of human vaginal xenografts in immunocompromised mice: development of a small animal model for the study of human immunodeficiency virus-1 infection. Am J Pathol 2001;159:2331–2345. [PubMed: 11733382]

Kreider JW, Howett MK, Wolfe SA, Bartlett GL, Zaino RJ, Sedlacek T, Mortel R. Morphological transformation in vivo of human uterine cervix with papillomavirus from condylomata acuminata. Nature 1985;317:639–641. [PubMed: 2997616]

Kumar AR, Snyder JM. Differential regulation of SP-A1 and SP-A2 genes by cAMP, glucocorticoids, and insulin. Am J Physiol 1998;274:L177–185. [PubMed: 9486201]

Laudy JA, Wladimiroff JW. The fetal lung. 2: Pulmonary hypoplasia. Ultrasound Obstet Gynecol 2000;16:482–494. [PubMed: 11169336]

Malkinson AM. Primary lung tumors in mice as an aid for understanding, preventing, and treating human adenocarcinoma of the lung. Lung Cancer 2001;32:265–279. [PubMed: 11390008]

Maltais F, Seaborn T, Guay S, Piedboeuf B. In vivo tracheal occlusion in fetal mice induces rapid lung development without affecting surfactant protein C expression. Am J Physiol Lung Cell Mol Physiol 2003;284:L622–632. [PubMed: 12618424]

Mendelson CR, Acarregui MJ, Odom MJ, Boggaram V. Developmental and hormonal regulation of surfactant protein A (SP-A) gene expression in fetal lung. J Dev Physiol 1991;15:61–69. [PubMed: 1651967]

Mendelson CR, Boggaram V. Hormonal control of the surfactant system in fetal lung. Annu Rev Physiol 1991;53:415–440. [PubMed: 2042967]

Mercer BM, Goldenberg RL, Moawad AH, Meis PJ, Iams JD, Das AF, Caritis SN, Miodovnik M, Menard MK, Thurnau GR, Dombrowski MP, Roberts JM, McNellis D. The preterm prediction study: effect of gestational age and cause of preterm birth on subsequent obstetric outcome. National Institute of Child Health and Human Development Maternal-Fetal Medicine Units Network. Am J Obstet Gynecol 1999;181:1216–1221. [PubMed: 10561648]

Otto-Verberne CJ, Ten Have-Opbroek AA, De Vries EC. Expression of the major surfactant-associated protein, SP-A, in type II cells of human lung before 20 weeks of gestation. Eur J Cell Biol 1990;53:13–19. [PubMed: 2076699]

Peault B, Tirouvanziam R, Sombardier MN, Chen S, Perricaudet M, Gaillard D. Gene transfer to human fetal pulmonary tissue developed in immunodeficient SCID mice. Hum Gene Ther 1994;5:1131–1137. [PubMed: 7530495]

Pepe GJ, Ballard PL, Albrecht ED. Fetal lung maturation in estrogen-deprived baboons. J Clin Endocrinol Metab 2003;88:471–477. [PubMed: 12519892]

Phelps DS. Surfactant regulation of host defense function in the lung: a question of balance. Pediatr Pathol Mol Med 2001;20:269–292. [PubMed: 11486734]

Phelps DS, Floros J. Localization of pulmonary surfactant proteins using immunohistochemistry and tissue in situ hybridization. Exp Lung Res 1991;17:985–995. [PubMed: 1769356]

Phillips B, Gazet JC. Growth of human foetal tissue in mice treated with antilymphocyte serum. Nature 1969;222:1292–1293. [PubMed: 4892650]

Piedboeuf B, Laberge JM, Ghitulescu G, Gamache M, Petrov P, Belanger S, Chen MF, Hashim E, Possmayer F. Deleterious effect of tracheal obstruction on type II pneumocytes in fetal sheep. Pediatr Res 1997;41:473–479. [PubMed: 9098847]

Pilewski JM, Panettieri RA Jr, Kaiser LR, Albelda SM. Expression of endothelial cell adhesion molecules in human bronchial xenografts. Am J Respir Crit Care Med 1994;150:795–801. [PubMed: 7522102]

Pilot-Matias TJ, Kister SE, Fox JL, Kropp K, Glasser SW, Whitsett JA. Structure and organization of the gene encoding human pulmonary surfactant proteolipid SP-B. DNA 1989;8:75–86. [PubMed: 2924687]

Puchelle E, Peault B. Human airway xenograft models of epithelial cell regeneration. Respir Res 2000;1:125–128. [PubMed: 11667974]

Schwarz MA, Zhang F, Lane JE, Schachtner S, Jin Y, Deutsch G, Starnes V, Pitt BR. Angiogenesis and morphogenesis of murine fetal distal lung in an allograft model. Am J Physiol Lung Cell Mol Physiol 2000;278:L1000–1007. [PubMed: 10781431]

Solarin KO, Ballard PL, Guttentag SH, Lomax CA, Beers MF. Expression and glucocorticoid regulation of surfactant protein C in human fetal lung. Pediatr Res 1997;42:356–364. [PubMed: 9284277]

Stahlman MT, Gray ME, Hull WM, Whitsett JA. Immunolocalization of surfactant protein-D (SP-D) in human fetal, newborn, and adult tissues. J Histochem Cytochem 2002;50:651–660. [PubMed: 11967276]

Tassler PL, Dellon AL, Canoun C. Identification of elastic fibres in the peripheral nerve. J Hand Surg [Br] 1994;19:48–54.

Vu TH, Alemayehu Y, Werb Z. New insights into saccular development and vascular formation in lung allografts under the renal capsule. Mech Dev 2003;120:305–313. [PubMed: 12591600]

Wang G, Christensen ND, Wigdahl B, Guttentag SH, Floros J. Differences in N-linked glycosylation between human surfactant protein-B variants of the C or T allele at the single-nucleotide polymorphism at position 1580: implications for disease. Biochem J 2003;369:179–184. [PubMed: 12356334]

Weaver TE, Whitsett JA. Processing of hydrophobic pulmonary surfactant protein B in rat type II cells. Am J Physiol 1989;257:L100–108. [PubMed: 2475034]

Witorsch RJ. Low-dose in utero effects of xenoestrogens in mice and their relevance to humans: an analytical review of the literature. Food Chem Toxicol 2002;40:905–912. [PubMed: 12065211]

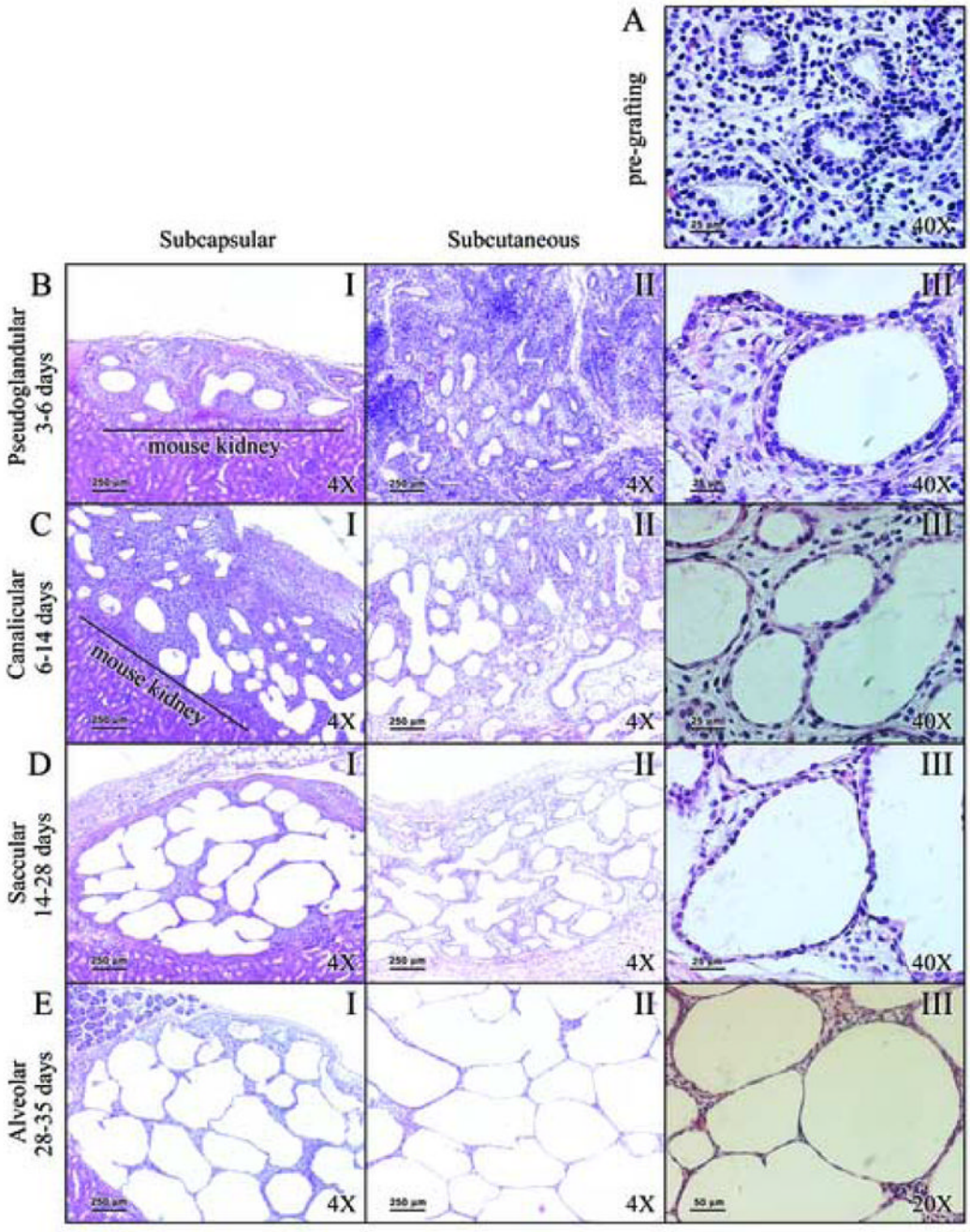

Figure 1. Both types of grafts recapitulate stages of *in utero* lung development

Panel A: Starting fetal lung tissue (16 weeks gestation). Panel B: Epithelial thinning and future air space enlargement seen after 3 days of grafting. Panel C: Grafts between 6 and 14 days show progression of differentiation. Panel D: Post 14 day grafts with flattening of epithelium. Panel E: Distended saccules with flattened epithelium are observed after 28 days of grafting. Panel A is characteristic of pseudoglandular stage of development. Changes in Panel B are consistent with the late pseudoglandular stage. In Panel C grafts resemble the canalicular stage of development, forming acini and increased number of capillaries. In Panel D grafts resemble saccular stage of *in utero* development display flattening of the epithelium, and differentiation of pre-Type II cells into Type II cells, and further differentiation onto Type I cells. Alveolar

spaces are considerably enlarged, and prominent alveolar septation is evident. In Panel E, differentiation of the epithelium to Type I cells, thinning of alveolar walls, and neovascularization are observed. Legend: I: low magnification (4×) of subcapsular grafts; II: low magnification (4×) of subcutaneous grafts; III: high magnification (A, B, C, and D at 40×; E at 20×) of subcutaneous grafts.

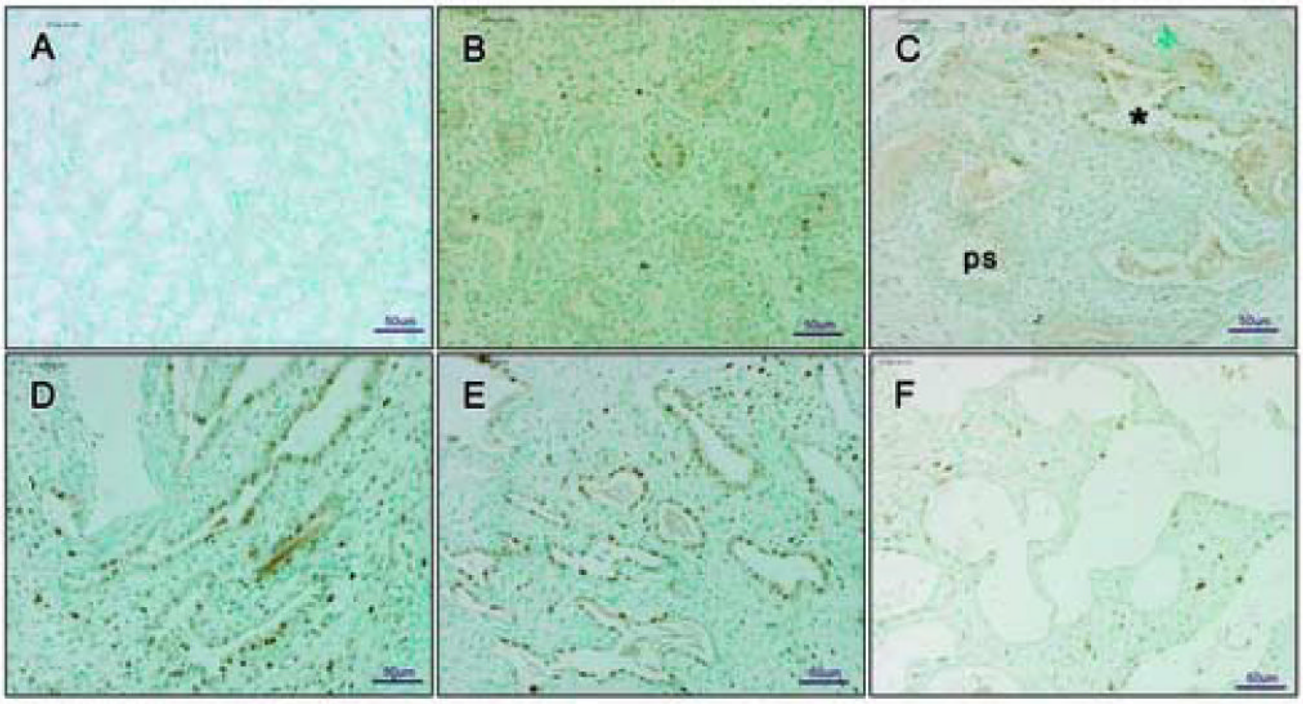

Figure 2. Cellular proliferation during graft development shown by ICC of PCNA

Panel A: negative control - mouse kidney of subcapsular graft. Panel B: limited PCNA immunopositive cells at 16 weeks development. Panel C: 6 day graft with majority of PCNA immunopositive cells in cannalicular stage of development (marked with *). Panel D and Panel E: 10 and 14 day grafts, respectively, abundant with PCNA immunopositive cells. Panel F: 21 day graft. In Panel A there is no staining within mouse tissue section. No brown cells are detectable indicating complete inhibition of endogenous peroxidase and lack of specific PCNA staining. Therefore, the PCNA positive cells in the other sections are of human and not mouse origin. In Panel C, PCNA immunopositive cells were observed within the tissue sections entering the cannalicular stage of development (marked with *), rather than those still in pseudoglandular stage (marked ps). In Panel D and E changes in the morphology of tissue are represented by the increasing number of PCNA immunopositive cells. Panel F shows a 21 day graft entering the saccular stage of development with sparsely distributed PCNA positive cells. Pseudoglandular and cannalicular stages are defined in Figure legend 1. Figures are representative of three experiments. All pictures are at 20× magnification.

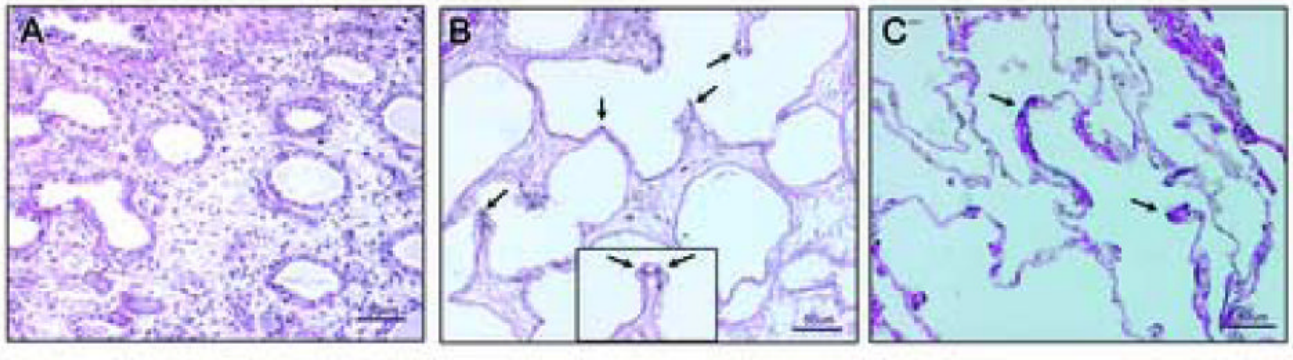

Figure 3. Elastic fiber proliferation is detectable in saccular stage

Panel A: 6 day graft lacking elastic fiber staining as would be expected in pseudoglandular/ cannalicular stage of development. Panel B: 14 day graft with elastic fibers visible as black punctate dots (arrows) at the tips of developing alveolar crests. Panel C: adult lung tissue (positive control) has an abundance of layered elastic fibers within the thin alveolar walls (arrows). The inset in panel B (dotted line) shows a high magnification (40×) of an alveolar crest with elastic staining (arrows). Hardly any staining was observed in 21 day graft (not shown). There is an abundance of collagen fibers in all tissues (red). Figures are representative of three experiments. Panels A, B, and C are at 20× magnification.

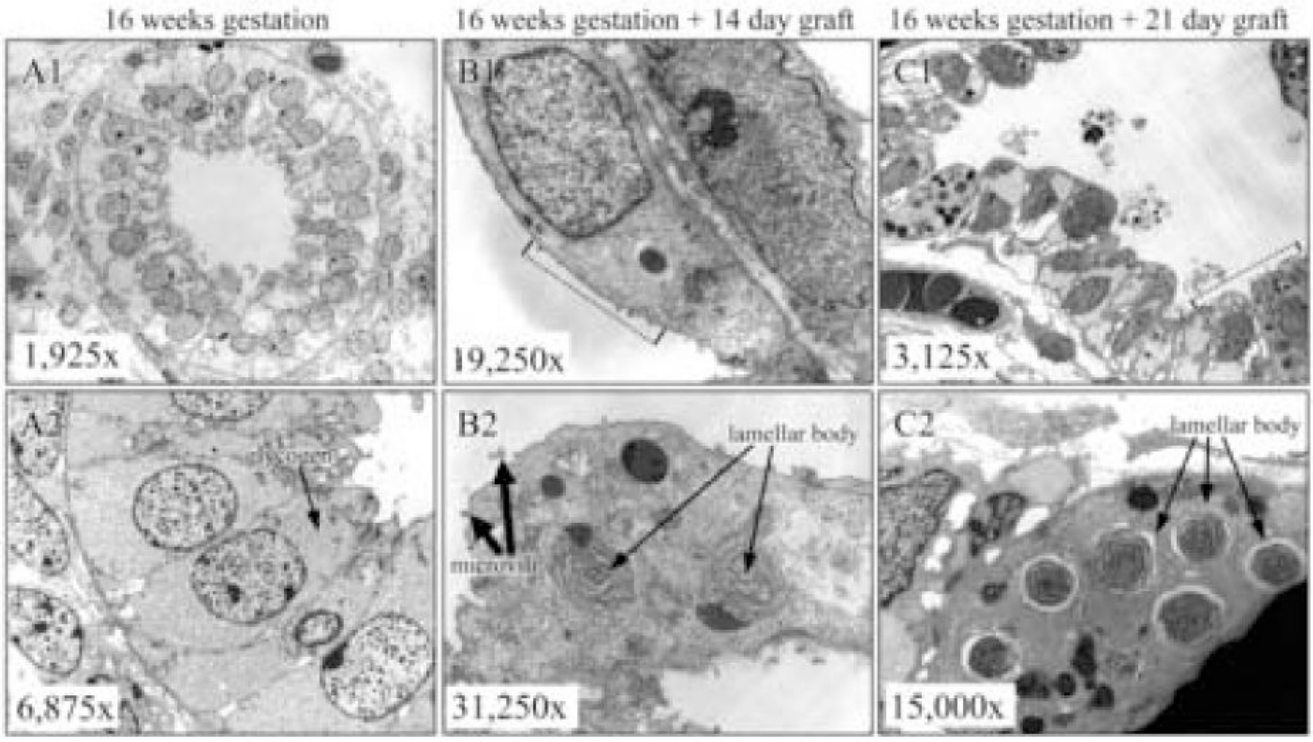

Figure 4. Lamellar bodies found in grafts, consistent with *in utero* development

Panel A1 and A2: Lamellar bodies are absent in starting fetal lung tissue. Pre- Panel B1 and B2: Lamellar bodies are first seen in 14 day grafts. Panel C1 and C2: 21 days post-grafting, the number of lamellar body positive cells and lamellar bodies per cell is sharply increased. (first 60 characters). In Panel A, Pre-Type II columnar cells are rich with glycogen. As shown in Panel B, 14 day grafts grafts are in early saccular stage of development, as evidenced by flattening of epithelial cells and scarce microvilli. In Panel C, numerous secreted lamellar bodies are seen in the alveolar spaces, but no tubular myelin-like structures are observed.

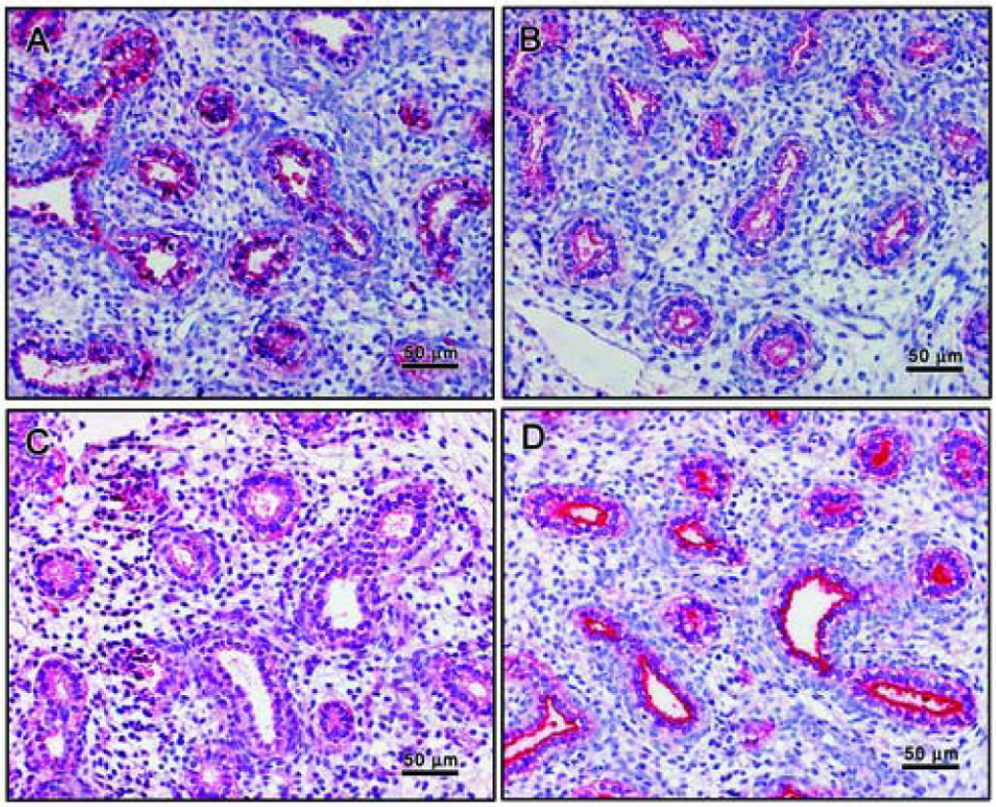

Figure 5. Surfactant proteins are present in starting tissues as shown by ICC

The primordia of alveoli are lined by cuboidal pre-type II cells that are immunopositive for SPs. Localization of SP-A (Panel A), SP-B (Panel B), and SP-C (Panel C) is uniform within the cells. Localization of SP-D (Panel D) is limited to the apical surface of the cells. Panels are shown at medium magnification (20×).

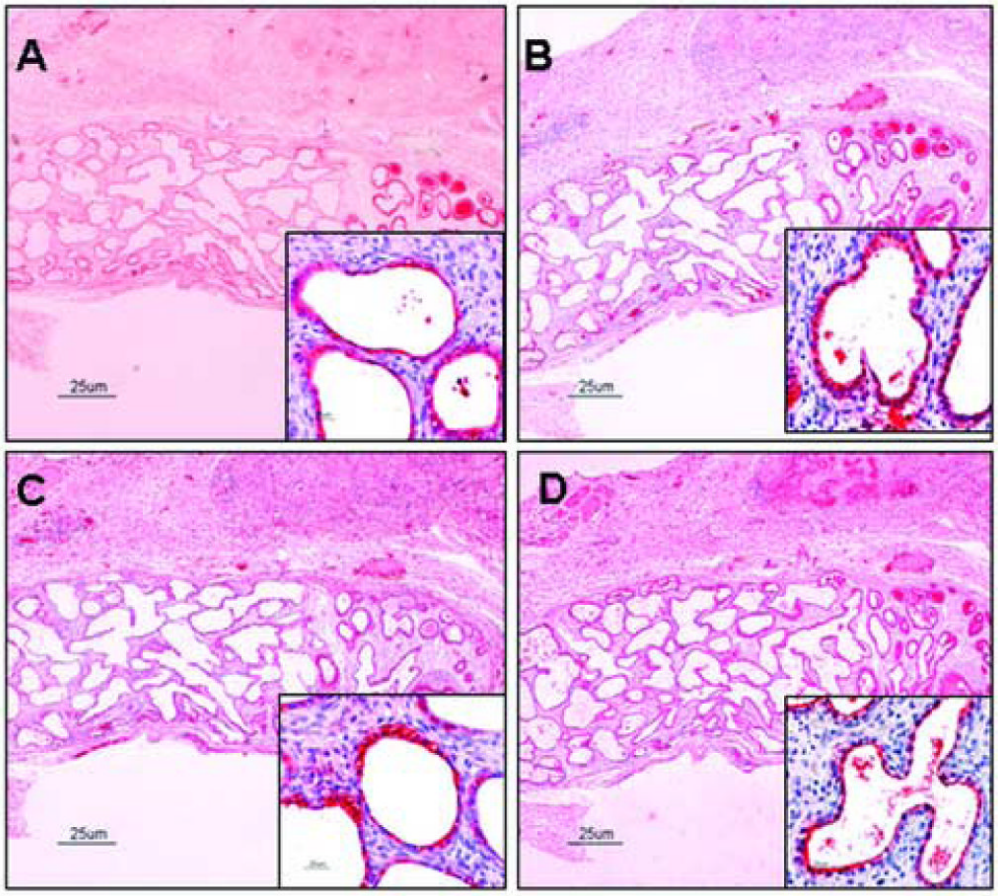

Figure 6. Surfactant proteins are present during graft development by ICC

Surfactant proteins are abundant in 21 day grafts shown in Figure. Immunostaining for SP-A is presented in Panel A, for SP-B in Panel B, for SP-C in Panel C, and for SP-D in Panel D. Localization of SP-A, SP-B, and SP-C (insert) is uniform within the cell. Localization of SP-D is limited to the apical surface of the cells (insert). After longer periods of grafting, cyto-differentiation is observed and fewer cells found to stain positive for surfactant proteins. This would be expected in a developing epithelium, where immuno positive pre-Type II cells are differentiating into Type II cells (immuno positive) which can then become Type I cells (immuno negative) (not shown). Panels are shown in low magnification (4×) and inserts are in high magnification (40×).

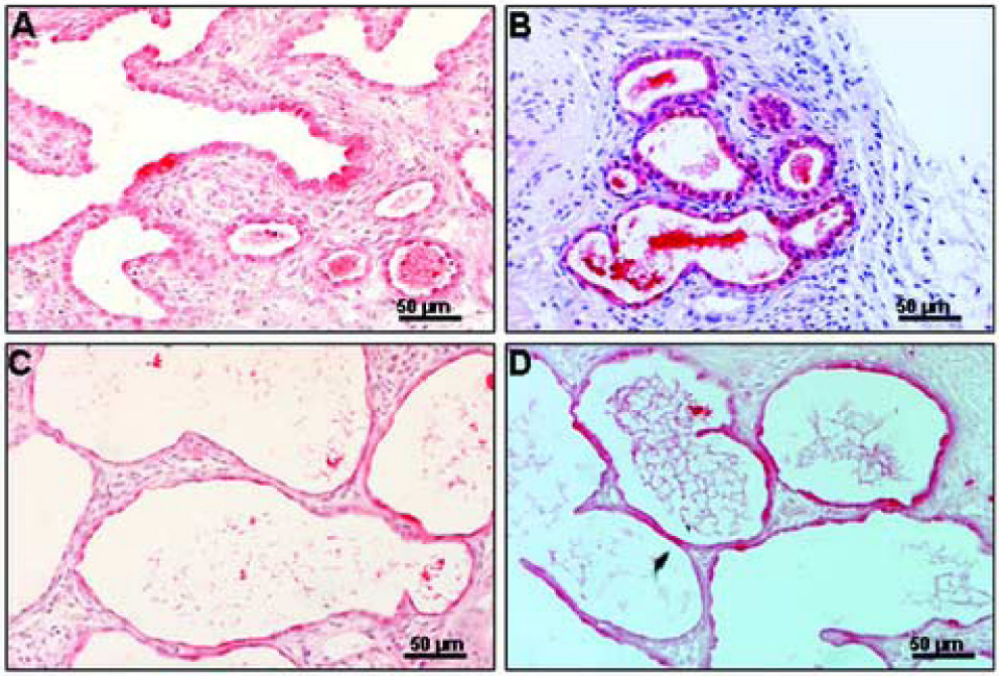

Figure 7. SP-A is present throughout graft development by ICC

Panel A: 6 day graft with pre-type II cuboidal cells immunopositive for SP-A. Panel B: 10 day graft with thinning epithelial cells predominantly SP-A immunopositive. Panel C: 14 day graft with saccular-like structures and differentiation of pre-type II into type II cells (both SP-A immunopositive). Panel D: 28 day graft with thinning saccules and septae. Panels shown at medium magnification (20×).

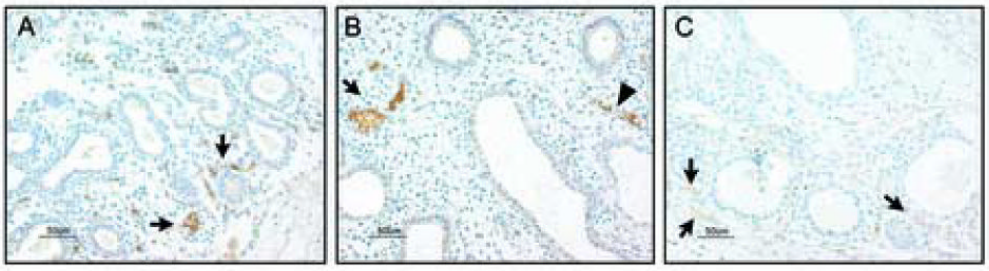

Figure 8. Human PECAM-1 is detectable by immunocytochemistry in early stage grafts

Panel A: Presence of blood vessels of human origin within the mesenchyme of a 3 day graft is indicated by PECAM-1 immunopositive cells (brown, arrows). Panel B: Branching of the PECAM-1 immunopositive clusters of cells (arrow) and formation of blood vessels (arrowhead) is evident in 6 day graft. Panel C: As differentiation progresses PECAM-1 staining becomes significantly fainter and mostly visible in the subpleural areas of the 14 day graft (as indicated by arrows). All panels are shown at medium magnification (20×).

Table 1

Primers used in the study

Oligo number	orientation	Gene specificity	Sequence from 5′ to 3′	Nucleotide position
780	S	SP-A	GACGTTTGTGTTGGAAGCCCTGG	White et al.: 3603-3625 (White et al., 1985)
68A	AS (RT)	SP-A	TGCCACAGAGACCTCAGAGT	White et al: 6333-6352 (White et al., 1985)
781	AS	SP-A	GGTACCAGTTGGTGTAGTTCACAG	White et al: 5688-5711 (White et al., 1985)
1321	S	SP-A	AAGTACAACACATATGCCTAT	White et al.: 5612-5632 (White et al., 1985)
110	AS (RT)	SP-B	GAATTCACCAGTGGAAGTGACTCCCGAGG	Pilot-Matias et al: 9685-9715 (Pilot-Matias et al., 1989)
603	AS	SP-B	TGGCTGCCGGGATTTGCACA	Pilot-Matias et al: 3478-3497 (Pilot-Matias et al., 1989)
70A	S	SP-B	CAAAGCCTGGAGCAAGCATT	Pilot-Matias et al: 1484-1503 (Pilot-Matias et al., 1989)
172	S	SP-B	CTGGTCATCGACTACTTCCA	Pilot-Matias et al: 2591-2610 (Pilot-Matias et al., 1989)
189	AS	SP-B	CATACAGATGCCGTTTGAGTC	Pilot-Matias et al: 3447-3467 (Pilot-Matias et al., 1989)
86A	AS (RT)	SP-C	CGCGGATCCACAGAGGGCGAATGGAAA	Glasser et al.: 3327-3353 (Glasser et al., 1988)
1116	AS	SP-C	GCACCTCGCCACACAGGGAG	Glasser et al.: 2773-2792 (Glasser et al., 1988)
1108	S	SP-C	GATGGAATGCTCTCTGCAGG	Glasser et al.: 2650-2669 (Glasser et al., 1988)
1106A	AS	SP-C	AAATCAGGCTGCTTTATTCTG	Glasser et al.: 3210-3230 (Glasser et al., 1988)
915	S	SP-D	AGGAGCTGCAGGGCAAGCAG	Rust et al.: 843-862 (Rust et al., 1991)
825	S	SP-D	CTGGAAGCAGAAATGAAGAC	Rust et al.: 262-281 (Rust et al., 1991)
925	AS	SP-D	TCCCTTAGGGCCTGCGAGGC	Rust et al.: 1690-1709 (Rust et al., 1991)
961	AS (RT)	SP-D	GAGCTATACCACACTGGCTAAG	Rust et al.: 4473-4494 (Rust et al., 1991)

Legend: sense (S), antisense (AS); reverse transcription (RT)